Non-traditional reflection of internal waves from a sloping bottom, and the likelihood of critical reflection

Theo Gerkema[1] and Victor I. Shrira[2]

Received 27 December 2005; revised 13 February 2006; accepted 15 February 2006; published 25 March 2006.

[1] The problem of internal inertio-gravity wave reflection from an arbitrarily orientated uniform slope is solved in a linear setting and with Coriolis effects fully included; that is, the horizontal component ($\tilde{f}$) of the Earth rotation vector is taken into account. A new criterion is derived for critical reflection. The presence of $\tilde{f}$ creates a specific anisotropy: the criterion depends on the orientation of the bottom slope in the horizontal geographical plane, while it does not depend on the horizontal orientation of the incident wave. Using an empirical-based bottom-slope distribution, the probability of critical reflection is calculated for diurnal and semi-diurnal internal-tide bands, for a range of latitudes and for various values of stratification. The probability is largest near the inertial latitudes, i.e., when the internal tides are near-inertial. It is explained how the inclusion of $\tilde{f}$ gives significant changes in the probability near these latitudes, especially for weak stratification. **Citation:** Gerkema, T., and V. I. Shrira (2006), Non-traditional reflection of internal waves from a sloping bottom, and the likelihood of critical reflection, *Geophys. Res. Lett.*, *33*, L06611, doi:10.1029/2005GL025627.

1. Introduction

[2] Reflecting internal waves at a sloping bottom represent an important process in ocean dynamics; they can create locally unstable stratification leading to the formation of a front [*Gemmrich and van Haren*, 2001], and are thought to play a significant role in ocean mixing [*Garrett and St. Laurent*, 2002]. The latter effect is greatly enhanced when reflection is (near) critical [*Eriksen*, 1998], in which case the reflected wave becomes very intense; nonlinear effects, including wave breaking, are then likely to occur. Evidence of this intensification was shown by *Eriksen* [1982] in internal-wave spectra. A vivid view of the overturning induced by near-critical reflection was recently given in laboratory experiments [*Dauxois et al.*, 2004].

[3] As pointed out by *Eriksen* [1998], gentle slopes are disproportionately important for near-critical reflection and induced mixing, because most of the internal-wave energy lies in the low-frequency part of the internal-wave spectrum, which is associated with near-horizontal propagation.

[4] The main purpose of this paper is to investigate the likelihood of the occurrence of critical reflection in the real ocean, using typical parameter values and an empirical-based distribution of slopes.

[5] In the open ocean, topographic features lie predominantly in the relatively weakly stratified abyss. It was recently shown that the horizontal component of the Earth rotation vector (to whose effects we refer as non-traditional) strongly modifies the dynamics of low-frequency internal waves, especially for weak stratification [*Gerkema and Shrira*, 2005]. The problem of internal waves reflecting from a slope has not been solved before with non-traditional terms included; here we first derive the solution for linear internal waves reflecting from an arbitrarily orientated uniform slope. From this solution we obtain a new non-traditional criterion for critical reflection, which we then apply to estimate its likelihood for internal tides in the ocean.

2. Reflection From a Uniform Slope

[6] Consider an incident internal wave of the form

$$w = \exp i(kx + ly + mz + \sigma t),$$

which upon reflection from a slope $z = \alpha x + \beta y$ (x is the west-east coordinate, y is south-north), yields an outgoing wave

$$W = Q \exp i(Kx + Ly + Mz + \sigma t).$$

The problem is to find Q, K, L, M as functions of k, l, m and α, β. They follow from the requirements that (i) the normal velocity vanishes at the slope, and (ii), both the incident and reflected waves satisfy the dispersion relation for internal inertio-gravity waves. At the slope, the velocity components of the incident wave are proportional to

$$\exp i(kx + ly + m\{\alpha x + \beta y\} + \sigma t)$$

and those of the outgoing wave are proportional to

$$\exp i(Kx + Ly + M\{\alpha x + \beta y\} + \sigma t).$$

The boundary condition of zero normal velocity means that their superposition should vanish for all x, y (and t); for this to be possible, we must require

$$k + \alpha m = K + \alpha M\,; \quad l + \beta m = L + \beta M\,.$$

Writing $M = qm$ (q to be found), we obtain

$$K = k + \alpha(1 - q)m\,; \quad L = l + \beta(1 - q)m\,. \tag{1}$$

The problem has thus been reduced to finding just two coefficients: q and Q (as functions of k, l, m and α, β).

[1]Royal Netherlands Institute for Sea Research, Texel, Netherlands.
[2]Department of Mathematics, Keele University, Keele, UK.

0094-8276/06/2005GL025627$05.00

[7] The incident wave with wavevector (k, l, m) has to satisfy the dispersion relation for internal inertio-gravity waves. This relation follows from the momentum equations on the $f,\tilde{f}$-plane, i.e., with the non-traditional Coriolis terms included [see, e.g., *Leblond and Mysak*, 1978; *Gerkema and Shrira*, 2005], combined with the equations for conservation of mass and energy. The resulting dispersion relation is

$$Al^2 + 2Blm + Cm^2 + Dk^2 = 0\,. \tag{2}$$

with $A = N^2 - \sigma^2 + \tilde{f}^2$, $B = f\tilde{f}$, $C = f^2 - \sigma^2$ and $D = N^2 - \sigma^2$ [*LeBlond and Mysak*, 1978, equation 8.46]. Here N denotes the buoyancy frequency; $f = 2\Omega \sin \phi$ and $\tilde{f} = 2\Omega \cos \phi$, where Ω is the Earth's angular velocity and ϕ the latitude. (In the so-called Traditional Approximation, the terms with $\tilde{f}$ are neglected.)

[8] The outgoing wave, with wavevector (K, L, M), too has to satisfy the dispersion relation (2). This requirement yields a quadratic equation for q whose roots are $q = 1$ (this obviously is not the one we are looking for; it represents a wave going through the sloping bottom), and

$$q = \frac{A(l+\beta m)^2 + D(k+\alpha m)^2}{m^2\left(A\beta^2 + D\alpha^2 - 2B\beta + C\right)}. \tag{3}$$

The amplitude factor Q of the outgoing wave is obtained by requiring $w + W = \alpha\,(u + U) + \beta\,(v + V)$ at the slope $z = \alpha x + \beta y$, thereby imposing the boundary condition. The horizontal velocity components can be expressed in terms of the vertical ones by using the momentum equations as given by, for example, *Gerkema and Shrira* [2005]; this yields

$$u = \bar{u}(k,l,m)w\,; \qquad v = \bar{v}(k,l,m)w,\,;$$

$$U = \bar{u}(K,L,M)W\,; \quad V = \bar{v}(K,L,M)W,$$

where $\bar{u}(k, l, m)$ and $\bar{v}(k, l, m)$ are given by

$$\bar{u} = -\frac{l\left(\tilde{f}l + fm\right) + i\sigma km}{i\sigma(k^2 + l^2)}\,; \quad \bar{v} = \frac{k\left(\tilde{f}l + fm\right) - i\sigma lm}{i\sigma(k^2 + l^2)}.$$

Using these expressions, the resulting Q is found to be

$$Q = -\frac{\alpha\bar{u}(k,l,m) + \beta\bar{v}(k,l,m) - 1}{\alpha\bar{u}(K,L,M) + \beta\bar{v}(K,L,M) - 1}. \tag{4}$$

With formulae (3) and (4), the description of the outgoing wave is complete.

3. Criterion for Critical Reflection

[9] By definition, critical reflection occurs when the group-velocity vector of the reflected wave is parallel to the bottom slope. This happens when $|q| \to \infty$, since, with (1), we find that the wavevector (K, L, M) then becomes parallel to the normal of the slope, $(-\alpha, -\beta, 1)$. This implies that the group-velocity vector, being perpendicular to the wavevector, indeed lies in the plane of the slope. (A laborious inspection shows that $|q| \to \infty$ coincides with $|Q| \to \infty$, as it should.)

[10] For $|q|$ to become infinite, the denominator in (3) must vanish:

$$A\beta^2 + D\alpha^2 - 2B\beta + C = 0. \tag{5}$$

This is the new criterion for critical reflection.

[11] For later convenience, we write $\alpha = \gamma \cos \nu$ and $\beta = \gamma \sin \nu$, where ν denotes the horizontal orientation of the slope, and γ its steepness. Without loss of generality, we can assume $\gamma \geq 0$. From (5), we then find an expression for the critical slope:

$$\gamma = \frac{B\sin\nu + \left[(B\sin\nu)^2 - C\left(A\sin^2\nu + D\cos^2\nu\right)\right]^{1/2}}{A\sin^2\nu + D\cos^2\nu}\,. \tag{6}$$

Remarkably, the critical slope does not depend on the zonal orientation of the incident wavevector, although it does depend on slope orientation ν, implying anisotropic behaviour in the x, y-plane. Under the Traditional Approximation, by contrast, we would have $B = 0$ and $A = D$, and hence isotropy; (6) then reduces to the well-known traditional criterion, see (8), with $\tilde{f} = 0$.

4. Probability of Critical Reflection

[12] A brief look at any topographic map of the ocean makes clear that slopes are overwhelmingly gentle. To illustrate this in a more quantitative way, we use the database of *Smith and Sandwell* [1997]. In this database, (square) cells have a longitudinal width of 1/30° at all latitudes; as a consequence, the cell size decreases from 3.7 × 3.7 km at the equator down to 1.1 × 1.1 km at 72°. This is noticeably smaller than the typical horizontal scale of an internal-tide beam (for example, the observations by *Pingree and New* [1991], give a scale of about 10km), and so, the database can be considered appropriate for our purposes. (We note that the database is based on depth soundings as well as gravity anomalies; the latter taken alone imply a somewhat coarser resolution than is suggested by the actual gridding.)

[13] Combining data from a number of sections (as detailed in the figure caption), we obtain the slope distribution shown in Figure 1; as usual, the distribution has been normalized such that the total enclosed area equals one. (We note that the distribution extends further to the right than shown in Figure 1.) Figure 1 demonstrates that slopes are mostly gentle; in fact, 67% of the slopes is less than 0.02.

[14] As an aside, we notice that the distribution is not Gaussian, but is rather closer to a Cauchy type distribution; for a really satisfactory fit, one has to resort to less common types, such as the thick curve in Figure 1, showing a Burr distribution [see, e.g., *Stuart and Ord*, 1994, p. 248].

[15] We now proceed as follows. First, we select a certain frequency interval $[\sigma_1, \sigma_2]$, for example, $[O_1, K_1]$ (diurnal tides), or $[N_2, S_2]$ (semi-diurnal tides). Then, for a certain latitude ϕ, stratification N, and slope orientation ν, we employ (6) to determine the range of critical slopes $[\gamma_1, \gamma_2]$ that corresponds to this frequency range; here $\gamma_{1,2} = \gamma(\sigma_{1,2}, \phi, N, \nu)$. Using a given slope distribution $D(\gamma)$, as illustrated in Figure 1, we finally obtain the probability of

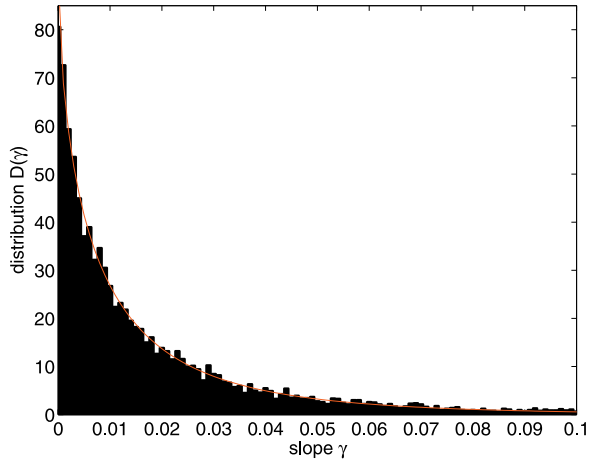

Figure 1. Slope distribution derived from the database of *Smith and Sandwell* [1997]. Here the bar width is $\Delta\gamma = 0.001$. This distribution is based on data from four sections: south-north sections at 180°W, and 30°W, as well as west-east sections at 10°S and 22°N (Atlantic Ocean, including the continental shelves). The thick curve shows a fit using a Burr distribution $a(1 + \gamma^b)^{-c}$, with $a = 91$, $b = 0.65$ and $c = 25$.

encountering the range of critical slopes, i.e., the probability of critical reflection:

$$P_\nu = \int_{\gamma_1}^{\gamma_2} d\gamma\, D(\gamma). \tag{7}$$

On averaging over all slope orientations ν, we obtain

$$P = \frac{1}{2\pi}\int_0^{2\pi} d\nu\, P_\nu.$$

(Under the Traditional Approximation the dependence on slope orientation ν disappears; then it suffices to calculate the probability for just one slope orientation.)

[16] We plot results for a range of latitudes, up to the latitude where the lower bound of the frequency range matches the local Coriolis parameter f (inertial latitude); this latitude is 27.6° for the diurnal range $[O_1, K_1]$, and 71.0° for the semi-diurnal range $[N_2, S_2]$ (see Table 1). The probability P for the diurnal range $[O_1, K_1]$ is shown in Figure 2; in the three panels, stratification N increases downward. The probability decreases steadily toward the equator; the lower the latitude, the steeper the slope must be to result in critical reflection, and such steep slopes are relatively rare (see Figure 1). Probabilities below 24° are very small, and are therefore not shown.

[17] It is clear from Figure 2 that at sufficiently low latitudes (e.g., 24°), the probability increases with increasing N. This is because internal-wave energy propagates less steeply for higher N, so they match more and more the abundant gentle slopes needed for critical reflection. In the immediate vicinity of the inertial latitude, however, the probability decreases with increasing N. This is because the lower bound O_1 already matches the gentle slopes, while the upper bound K_1 becomes less steep for higher N; as a result, the contribution from critical reflection from steeper slopes is more and more lost as N increases.

Table 1. Diurnal and Semi-Diurnal Tidal Frequencies and Corresponding Inertial Latitudes

Constituent	Frequency, rad/s	Inertial Latitude
O1	0.000067598	27.6°
K1	0.000072921	30.0°
N2	0.00013788	71.0°
M2	0.00014052	74.5°
S2	0.00014544	85.8°

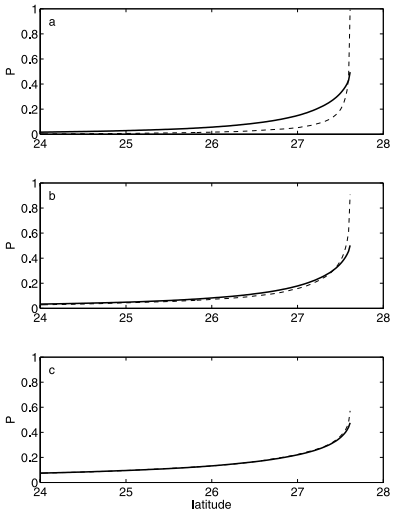

Figure 2. Probability of critical reflection for the diurnal frequency range $[O_1, K_1]$, as a function of latitude. The dashed line shows the result obtained under the Traditional Approximation ($\tilde{f} = 0$); the solid line shows the non-traditional result. Various values of N are used: a) 2×10^{-4}; b) 5×10^{-4}; c) 2×10^{-3}rad/s.

[18] Overall, we see in each panel that the highest probability occurs near the inertial latitude, i.e., for near-inertial frequencies. An entirely similar result is found for the semi-diurnal range $[N_2, S_2]$, see Figure 3, except that the inertial latitude for the lower bound now lies, of course, much higher.

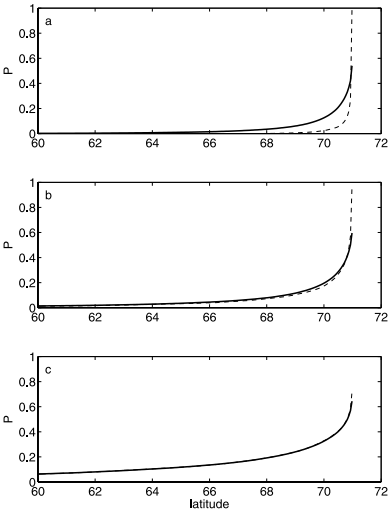

Figure 3. As in Figure 2, but now for the semi-diurnal range frequency $[N_2, S_2]$.

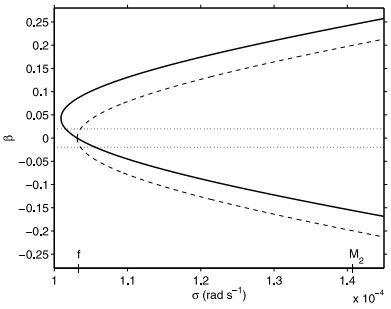

Figure 4. Critical slopes $\gamma = \pm\beta$ as a function of wave frequency σ, at fixed latitude $\phi = 45°$N and for stratification $N = 5 \times 10^{-4}$ rad/s. The upper half covers critical slopes γ orientated northward ($\nu = \pi/2$, hence $\beta = \gamma$); the lower half, slopes orientated southward ($\nu = -\pi/2$, hence $\beta = -\gamma$). The region between the horizontal dotted lines indicates 67% slope coverage (see Figure 1). The solid line gives the non-traditional curve, while the dashed one is obtained under the Traditional Approximation. [After *Gerkema and Shrira*, 2005].

[19] The curves plotted in Figures 2 and 3 are in essence a map of the distribution $D(\gamma)$ shown in Figure 1. This can be seen most easily by considering a narrow frequency range $[\sigma, \sigma + \delta\sigma]$. The integral in (7) then reduces to

$$P_\nu = D(\gamma(\sigma, \phi, N, \nu)) \frac{\partial \gamma}{\partial \sigma} \delta\sigma \,.$$

Apart from the averaging over ν, we now see that the variation of P with latitude ϕ, is given by the distribution D via the dependence of γ on ϕ (multiplied by the factor $\partial\gamma/\partial\sigma$, which also depends on ϕ).

5. The Role of $\tilde{f}$

[20] Figures 2 and 3 show clear differences between the traditional result ($\tilde{f} = 0$, dashed line) and the non-traditional one ($\tilde{f}$ included, solid line). In line with the conclusions drawn by *Gerkema and Shrira* [2005], non-traditional effects are most noticeable for near-inertial waves, and for weak stratification.

[21] From Figures 2 and 3 follows that non-traditional effects increase the probability of critical reflection at low latitudes (in other words, for wave frequencies sufficiently high with respect to $|f|$, the inertial frequency), and lower it in the immediate vicinity of the inertial latitude. This behaviour is most readily explained by considering purely latitudinal slopes, i.e., $\nu = \pm\pi/2$, so $\alpha = 0$ and $\beta = \pm\gamma$; the slope now equals β (or $-\beta$ if $\nu = -\pi/2$). For a fixed latitude and stratification ($\phi = 45°$N, $N = 5 \times 10^{-4}$ rad/s), we show β as a function of wave frequency σ in Figure 4.

[22] For any band of frequencies outside the vicinity of f, we see that $\tilde{f}$ causes the critical slope to be less steep for $\nu = -\pi/2$, and steeper for $\nu = \pi/2$. This can also be seen by making a Taylor expansion of (6) about $\tilde{f} = 0$, which gives

$$\gamma = \left(\frac{\sigma^2 - f^2}{N^2 - \sigma^2}\right)^{1/2} + \frac{f\tilde{f}\sin\nu}{N^2 - \sigma^2} + \cdots . \qquad (8)$$

This expression confirms that $\tilde{f}$ decreases the steepness of the critical slope for $\nu = -\pi/2$, while increasing it for $\nu = \pi/2$. Since the slope-distribution $D(\gamma)$ is a decreasing function (see Figure 1), the former outweighs the latter, and hence $\tilde{f}$ increases the overall probability of critical reflection.

[23] However, if we consider a frequency band $[f, f + \delta]$, we see that the range of gentle critical slopes covered by the traditional curve (dashed line) is larger than that covered by the non-traditional curve (solid line). This explains why the probability is in that case larger under the Traditional Approximation, and this is reflected in Figures 2 and 3 in the vicinity of the inertial latitude.

[24] Finally, we note that since the inclusion of $\tilde{f}$ gives rise to an enlargement of the frequency range (as is clearly visible in Figure 4), critical reflection can now also occur at sub-inertial frequencies. (This range was not included in Figures 2 and 3, because an average over all angles ν was taken, and the width of the range is different for different angles; in fact, it vanishes for $\nu = 0, \pi$.)

6. Discussion

[25] The expressions derived in Sections 2 and 3, which we applied here to internal-tide frequency bands, are quite general and can be applied to any part of the internal inertio-gravity spectrum, in various contexts. In fact, by considering a range of latitudes, we also covered the near-inertial band, in this case at the inertial latitudes of O_1 and N_2. The results show that critical reflection is indeed most likely to occur at near-inertial frequencies. (This is the case both with and without the Traditional Approximation, despite the differences between the two.) From an oceanographic point of view this is particularly interesting because internal-wave spectra usually show a strong peak at the inertial frequency [e.g., *Fu*, 1981]; it is the most energetic part of the spectrum.

[26] The empirical-based distribution of slopes used in this paper (Figure 1) is well described by a Burr distribution, except perhaps in the tail, where the fit is less reliable because it involves relatively few data points. (On theoretical grounds, one might expect the tail to be given by a Poisson distribution.) However, the precise behaviour of the tail need not concern us here, for two reasons. First, the probability of steep slopes is in any case very small. Second, to have critical reflection at steep slopes, the wave frequency needs to be relatively high. Since high-frequency internal waves form the least energetic part of the internal-wave spectrum (cf. the Garrett-Munk spectrum [e.g., *Munk*, 1981]), this reinforces the conclusion that the tail is of little importance from a global energetics perspective. However, if we were interested in a particular high-frequency band of the internal-wave field, then the details of the tail would be essential for the redistribution of energy between different scales.

[27] The restriction to uniform slopes, adopted in this paper, precludes effects of convexity. They may be important for internal wave reflection and mixing; for example, *Gilbert and Garrett* [1989] argued that mixing is more likely for convex than for concave slopes. On the other hand, if we allow for multiple reflections, then waves reflected from a supercritical segment of a concave bottom feature may eventually experience critical reflection. This issue requires further study.

[28] In this paper we considered just the occurrence of critical reflection. For a proper description of the actual process of critical reflection, nonlinear and viscous effects need to be included [see, e.g., *Dauxois and Young*, 1999]. The issue of its integral impact on the energy balance and mixing in the deep ocean requires further study. At the moment we are not aware of oceanographic data which would unambiguously link enhanced mixing to critical reflection of internal tides; one of our conclusions is that we can now focus the search to vicinities of the inertial latitudes (given in Table 1 for each of the tidal components). We might expect more clear-cut manifestations at inertial latitudes for the semi-diurnal band, i.e., around 70–75° and around 86°, where there will be no interference with enhanced mixing due to subharmonic resonance (in contrast to the region near 30°).

[29] **Acknowledgments.** The first author is financially supported by the NWO/ALW program CLIMA-DIM. We thank Hans van Haren for comments on an earlier version of this paper, and John Preater for the suggestion to use the Burr family of distributions, and for helpful discussion on the nature of the tails of the slope distributions.

References

Dauxois, T., and W. R. Young (1999), Near-critical reflection of internal waves, *J. Fluid Mech.*, *390*, 271–295.

Dauxois, T., A. Didier, and E. Falcon (2004), Observation of near-critical reflection of internal waves in a stably stratified fluid, *Phys. Fluids*, *16*, 1936–1941.

Eriksen, C. C. (1982), Observations of internal wave reflection off sloping bottoms, *J. Geophys. Res.*, *87*, 525–538.

Eriksen, C. C. (1998), Internal wave reflection and mixing at Fieberling Guyot, *J. Geophys. Res.*, *103*, 2977–2994.

Fu, L. L. (1981), Observations and models of inertial waves in the deep ocean, *Rev. Geophys.*, *19*, 141–170.

Garrett, C., and L. St. Laurent (2002), Aspects of deep ocean mixing, *J. Oceanogr.*, *58*, 11–24.

Gemmrich, J. R., and H. van Haren (2001), Thermal fronts generated by internal waves propagating obliquely along the continental slope, *J. Phys. Oceanogr.*, *31*, 649–655.

Gerkema, T., and V. I. Shrira (2005), Near-inertial waves in the ocean: Beyond the 'traditional approximation', *J. Fluid Mech.*, *529*, 195–219.

Gilbert, D., and C. Garrett (1989), Implications for ocean mixing of internal wave scattering off irregular topography, *J. Phys. Oceanogr.*, *19*, 1716–1729.

LeBlond, P. H., and L. A. Mysak (1978), *Waves in the Ocean*, 602 pp., Elsevier, New York.

Munk, W. (1981), Internal waves and small-scale processes, in *Evolution of physical oceanography*, edited by B. A. Warren and C. Wunsch, pp. 264–291, MIT Press, Cambridge, Mass.

Pingree, R. D., and A. L. New (1991), Abyssal penetration and bottom reflection of internal tidal energy in the Bay of Biscay, *J. Phys. Oceanogr.*, *21*, 28–39.

Smith, W. H. F., and D. T. Sandwell (1997), Global sea floor topography from satellite altimetry and ship depth soundings, *Science*, *277*, 1956–1962.

Stuart, A., and J. K. Ord (1994), *Kendall's Advanced Theory of Statistics*, vol. 1, 676 pp., Edward Arnold, London.

T. Gerkema, Royal Netherlands Institute for Sea Research, P.O. Box 59,1790 AB Den Burg, Texel, Netherlands. (gerk@nioz.nl)

V. I. Shrira, Department of Mathematics, Keele University, Keele ST5 5BG, UK.